Ultramicroscopy 276 (2025) 114201

Contents lists available at ScienceDirect

Ultramicroscopy

journal homepage: www.elsevier.com/locate/ultramic

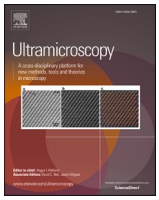

TEM-EDS microanalysis: Comparison between different electron sources, accelerating voltages and detection systems

Roberto Conconi [a,b,*], María del Mar Abad Ortega [c], Fernando Nieto [d], Paolo Buono [e], Giancarlo Capitani [a,*]

[a] Department of Earth and Environmental Sciences, University of Milano-Bicocca, Piazza della Scienza 4, Milano 2016, Italy
[b] Université de Lille, CNRS, INRAE, Centrale Lille, UMR 8207-UMET-Unité Matériaux et Transformations, Lille F-59000, France
[c] Centro de Instrumentación Científica, Universidad de Granada, Paseo Prof. Juan Ossorio s/n, Granada, 18071, Spain
[d] Departamento Mineralogia y Petrologia and IACT, Universidad de Granada, Avenida Fuente Nueva s/n, Granada 18071, Spain
[e] Department of Computer Science, University of Bari, Via Orabona 4, Bari 70125, Italy

ARTICLE INFO

Keywords:
Transmission electron microscopy
Energy dispersive spectroscopy
X-ray microanalysis
Absorption correction

ABSTRACT

Two TEM-EDS quantification methods based on standards of known compositions, namely the Cliff and Lorimer approximation and the absorption correction method based on electroneutrality are employed and the results obtained with three different TEMs and EDS systems, compared. The three TEM instruments differ in source type (field emission vs. thermionic), accelerating voltage (200 vs. 300 kV) and EDS system type (4 in-column silicon drift detector (SDD) vs. single SDD). We found that EDS calibration appears to be "strictly instrument specific", i.e., no universally valid *k*-factors can exist, but only *k*-factor sets for a specific combination of microscope and EDS system. As expected, 4-in column SDD systems, because of their larger sensitive areas compared to classical single SDD, are more efficient in data collection and, therefore, have lower detection limits. However, other sources of error may influence the final output, sometimes subverting the expectations. EDS analyses performed with FEG-TEMs exhibit lower radiation-induced migration of weakly bounded elements than TEMs equipped with a conventional source and lower beam current. This result may be explained by the smaller spot size used with the conventional TEM that in total led to a higher electron dose per sample atom. In addition, this work confirms that the absorption correction method is to be preferred whenever dealing with thick and/or dense samples, whereas the Cliff and Lorimer approximation, because simpler and faster, in all the other cases. Finally, we renew the necessity to determine two distinct $k_{O/Si}$ factors, one for lighter and one for denser compounds.

1. Introduction

Transmission electron microscopy (TEM) coupled with energy dispersive spectroscopy (EDS) is a well-established technique for obtaining morphological, microstructural, and compositional information at the sub-micrometre scale. EDS spectroscopy has become a standard option for every TEM because it is relatively easy to use, fast and of low acquisition costs compared to other TEM analytical techniques (i.e., electron energy loss spectroscopy, EELS). All elements, therefore also the geologically relevant ones, except for a few pathological overlaps and light elements such as H, He, and Li, can be reliably identified and quantified with a detection limit of around 0.1 wt %.

Because TEM samples are unavoidably very thin, typically tens of nm, the interaction volume between the beam and the sample is very small. As a result, the classical corrections applied in EDS microanalysis of bulk samples, known as *ZAF* correction [1], become negligible in TEM-EDS microanalysis. This assumption is known as the *thin foil criterion* [2].

TEM-EDS microanalysis, as well as EDS microanalysis of bulk samples in a scanning electron microscope (SEM), can operate without calibration against standards of known composition, unlike wave dispersive systems (WDS), for instance. In the truly *standardless method*, the X-ray emission of the targeted element is calculated from *first principles* [3,4]. This method has become very popular because it is fast, simple and the results are apparently similar to those obtained by the procedure with standards. However, in a companion paper, Conconi et al. [5] demonstrated how this method is less accurate than standard-based methods and how, in case of dense or thick samples, the

* Corresponding authors.
E-mail addresses: roberto.conconi@univ-lille.fr (R. Conconi), giancarlo.capitani@unimib.it (G. Capitani).

https://doi.org/10.1016/j.ultramic.2025.114201
Received 16 July 2024; Received in revised form 12 June 2025; Accepted 16 June 2025
Available online 17 June 2025

correction for absorption cannot be neglected.

In scientific literature, standard-based TEM-EDS microanalysis typically refers to the *Cliff-Lorimer approximation* [6] or, less commonly, to the *absorption correction method* [7]. However, as evidenced by Conconi et al. [5], the Cliff-Lorimer method, considering absorption negligible, may yield inaccurate results when working in thicker area of the sample or with dense samples. On the other hand, the absorption correction method, which for practical reasons relies on a quadratic function of the absorption (while a comprehensive treatment should include higher-order terms), may not yield accurate results for very high thickness. To address these limitations, alternative absorption correction methods have been developed in recent years, such as the *ζ-factor method* [8,9], the *thickness factor (T_F) and thickness correction coefficient (T_C) method* [10], and the *sum of squared residuals method* [11]. However, even these methods are not devoid of drawbacks. The *ζ-factor method* requires the knowledge of the beam current and cannot be used in TEMs devoid of Faraday cup or EELS. The *T_F and T_C method* requires the determination of the sample thickness profile and it is not of practical use for the varied and complex mineral compounds. The *sum of squared residuals method* assumes minerals as ideal compounds, which is almost never the case because of the presence of vacant sites (e.g. amphiboles), presence of the same element species in different sites (e.g. ^{IV}Al and ^{VI}Al), different oxidation states for the same element (e.g. Fe^{2+} and Fe^{3+}), and by admission of the authors themselves, this method is unsuitable for minerals having more than five ionic sites and element with different oxidation states.

In this paper, we aim to investigate and compare the application of the *Cliff-Lorimer approximation* and the *absorption correction method* across three TEM instruments that differ in source type (field emission vs. thermionic), accelerating voltage (200 vs. 300 kV) and EDS system type (4 in-column silicon drift detector (SDD) vs. single SDD), with all other variables held constant (standards, samples, operating conditions, etc.). This paper follows up a previous investigation on TEM-EDS microanalysis [5], where the procedure for *k*-factors calibration (for both absorption-corrected and non-corrected analyses) is described, the necessary theoretical background provided, and applications to well characterized mineral phases discussed. Moreover, a spreadsheet for the calculation of the thickness involved in the absorption correction was released. Here, the spreadsheet has been upgraded and released alongside this paper. In particular, the new spreadsheet allows more elements to be considered in the calculation of electron neutrality and provides the flexibility to change their valence. This feature is especially useful for calculations involving cations with variable valence, such as S and Fe, for instance, and it is also beneficial for hydroxylated minerals [12]. Since H is not detected by EDS (or WDS) systems, it is common practice to recalculate mineral compositions based on a reduced number of negative charges: 22 for micas (as in muscovite, $KAl_2AlSi_3O_{10}(OH)_2$), 28 for chlorite (as in clinochlore, $(Mg,Fe^{+2})_5Al(Si_3Al)O_{10}(OH)_8$), 46 for amphibole (as in tremolite, $Ca_2Mg_5Si_8O_{22}(OH)_2$), and so on. Although this method does not alter the measured cations proportions, when used with the TEM-EDS absorption correction method it may lead to physically unrealistic negative values of thicknesses calculated through the electron neutrality criterion. To overcome this problem, the new spreadsheet allows for the reduction of O valence to account for the contribution of H. In this way, the O valence in mica is reduced to –1.83 (reduced basis of negative charge/n. of oxygens = –22/12), in chlorite to –1.56 (–28/18), in amphibole to –1.92 (–46/24), and so on. Of course, after correcting for the absorption, the mineral formula must be recalculated on an integral basis of negative charges (i.e. –24 for micas, –36 for chlorite, –48 for amphibole, and so on).

2. Instruments and samples

The study was conducted at the Centre for Scientific Instrumentation (CIC) of the University of Granada. The analyses were obtained using a FEI TITAN G2 operated at 300 kV (hereafter TITAN) and a ThermoFisher Scientific TALOS F200X operated at 200 kV (hereafter TALOS). Both instruments are equipped with a field emission gun (FEG) Schottky source and a ThermoFisher 4 in-column SDD Super-X EDS with a windowless design, providing a total detection area of 120 mm^2 (30 mm^2 per detector). Each detector is mounted at a 45° angle respect to the x-tilt axis of the goniometer, and 90° apart from each other. The detector elevation angle is different between the two instruments: it is 18° for the TITAN and 22° for the TALOS, resulting in detection solid angles of 0.7 and 0.9 sr, respectively [13,14].

The data obtained at the CIC are compared with those recently obtained at the Platform of Microscopy of the University of Milano-Bicocca (PMiB) using a JEOL JEM 2100P operated at 200 kV (hereafter JEOL). The instrument is equipped with a conventional LaB_6 source and a windowless Oxford SDD UltimMax EDS detector with an 80 mm^2 sensor. The detector is mounted with an azimuthal angle of 90° (i.e., perpendicular to the x-axis of the goniometer) with an elevation angle of 22°, for a resulting detection solid angle of 0.5 sr. A special groove towards the EDS detector in the single tilt specimen holder used in the experiments minimizes penumbra effects and allows analyses at 0° x-tilt. A beryllium sample allocation and an insertable anti-scattering aperture along the beam path, both contribute to reduce the background noise of the spectrum.

Ion-milled TEM-mounts and powdered samples dispersed on holey-C Cu grids were employed. The formers were carbon coated with a 10 nm C film to avoid electrostatic charging during the measurements.

k-factors were derived for thirteen elements using sixteen different minerals and two synthetic compounds, all characterized by electron microprobe analyses (refer to Supplementary Material, Table S1). All *k*-factors were measured using the intensity extrapolated only from the Kα line. Spectra for EDS calibration were acquired in STEM (scanning–-transmission) mode using a selected area of 50×50 nm and an acquisition time of 50 s for all elements. Additionally, for Na and K, an acquisition time of 10 s was used in order to evaluate any radiation-induced migration commonly affecting these elements. The analyses were taken at 0-tilt orientation with the aim to warrant the same geometry for all standards and test samples, which in all cases corresponded to an orientation far from zone axis, but from phyllosilicates, which were prepared by ion milling from cleavage flakes glued on Cu rings, implying an orientation at 0-tilt close to [001]. The operative conditions were chosen according to common user analysis conditions and were kept constant for a given instrument along the entire calibration procedure. The nominal beam spot size was 5 nm for the TALOS and the TITAN and 3 nm for the JEOL. The measured beam currents during the analyses were 0.44, 0.60 and 0.91 nA for the JEOL, TALOS and TITAN, respectively.

TEM-EDS spectra were processed using the Aztec software (Oxford) for data collected with the JEOL and the Velox software (ThermoFisher Scientific) for data collected with both the TITAN and TALOS. These two programs use different approaches for processing spectra. Velox uses an empirical three-parameters Bethe-Heitler function to fit the background across the entire spectrum (Velox reference manual). Aztec does not subtract background but applies a top hat filter to the spectrum profiles of the unknown and of the reference standard [15]. For quantification with experimental *k*-factors, Velox uses deconvolution based on a maximum likelihood fit in which a family of lines is fitted as whole. Analogously, Aztec fits experimental peak profiles over the X-ray peaks of interest. Consequently, the relative error associated to the measure is calculated in a somewhat different way. In Velox the deconvolution error is combined with an error estimate for the cross-section models and, as a rule of thumb, an error of 20 % is assumed for the *k*-factors. In Aztec the relative error is estimated on the basis of counting statistics and an additional error is propagated according to a fitting parameter.

Therefore, to compare quantification results across all three instruments, avoiding any difference introduced by the different software, a third-party software, the HyperSpy Python library [16], was also used. Unlike commercial software, which often function as a "black box"

providing no full details on how spectra and compositions are computed, HyperSpy, being open source, offers much more control and transparency over the process. In HyperSpy background fitting was performed using a Bremsstrahlung model [17] and a least-squares fit function based on the Levenberg-Marquardt algorithm was used to extract intensities [18]. The relative error was obtained as $Er\ \% = \sigma_{NET}/I_{NET}*100$, where $\sigma_{NET} = [(I_{NET} + I_{BKG})/t + I_{BKG}/t]^{½}$ is the standard deviation of the net intensity (I_{NET}), I_{BKG} is the background intensity and t is the acquisition time (50 s). No other sources of error, as those arising from k-factors or from the cross section, were considered.

3. Results and discussion

3.1. k-factors

Generally, the trend of the k-factors (Fig. 1, Table S2) is similar across the three microscopes, showing an almost regular increase on both sides of Si, which is the reference element. Specifically, k-factors derived using the Cliff-Lorimer approximation (hereafter CLA factors) present similar values in all microscopes, with only a few exceptions such as higher values for P and S in the TITAN, and a lower value for Na in the TALOS. Conversely, the k-factors extrapolated at 0 thickness (ACM factors) show differences between different microscopes. The values of the JEOL and TITAN ACM-factors are comparable, whereas in the TALOS, elements on the low energy side of Si have higher values and those on the high energy side have lower values.

Since the k-factors are calculated as $k_{X/Si} = (C_X/C_{Si})*(I_{Si}/I_X)$ [5], where C_X and C_{Si} are the concentrations (weight % or atomic %) of elements X and Si in the sample, and I_X and I_{Si} are the measured intensities, respectively, the observation above could signify a lower sensitivity for the high energies and a lower sensitivity for low energies of the TALOS detector as compared with the other systems.

Another feature of the k-factor vs. Z plot is that the differences between the CLA- and ACM-factors are wider in the TALOS than in the TITAN and JEOL. At first sight, this observation indicates major absorption-related problems in the TALOS, especially for high energy X-ray photons (higher than the $Si_{K\alpha}$), than for the other TEMs and may depend, at least in part, on the same argument above. However, if a lower sensitivity for high energy photons were the only reason, one should expect systematically higher values of both factor types rather than a large difference between them. A possible explanation of the observed difference may rely on the electron beam interaction volume, higher at 200 kV because of the larger cross section, than at 300 kV (Fig. 2). The larger interaction volume, in turn, determines a larger volume involved in the absorption of X-rays within the sample, hence larger ACM-factors. In the JEOL, although the interaction volume is, in principle, the same as in the TALOS, the single SDD detector determines a smaller sample volume involved in the absorption of the X-rays, hence smaller ACM-factors.

In Fig. 3, we plot the I_K/I_{Si} vs. $I_K + I_{Si}$ intensities in muscovite. The data collected with the JEOL are more scattered than those collected with the TITAN and the TALOS, a trend that is analogous for all elements. At first sight, this effect can be explained by considering that the TITAN and the TALOS were operated with a beam current that was respectively 2.1 and 1.4 times larger than that of the JEOL. Moreover, both FEG instruments have 4 in-column sensitive SDD placed at the four

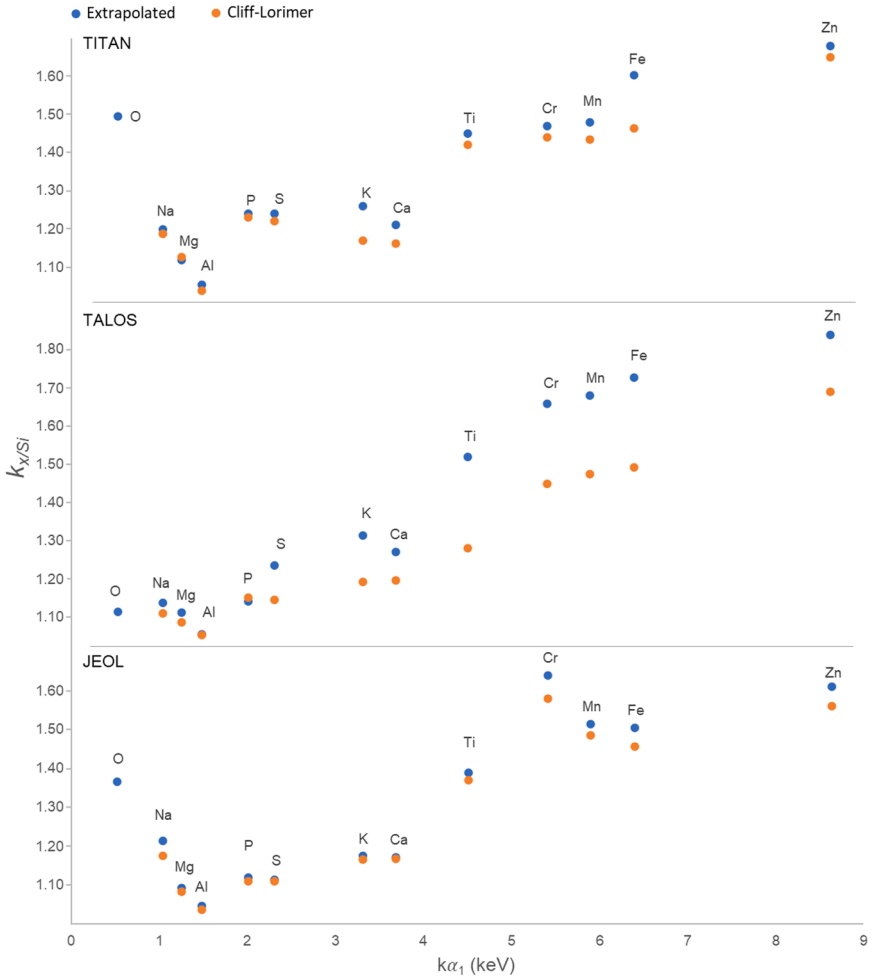

Fig. 1. Plot of the extrapolated at 0-thickness (blue dots) and Cliff-Lorimer (orange dots) $k_{X/Si}$ factors for the TITAN, TALOS and JEOL instruments.

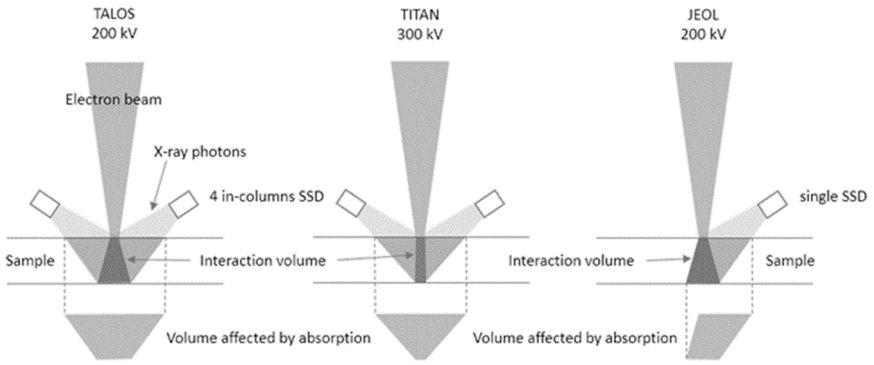

Fig. 2. Schematic representation of the interaction volume and of the volume of sample involved in the absorption of X-rays for the three different systems tested in the study.

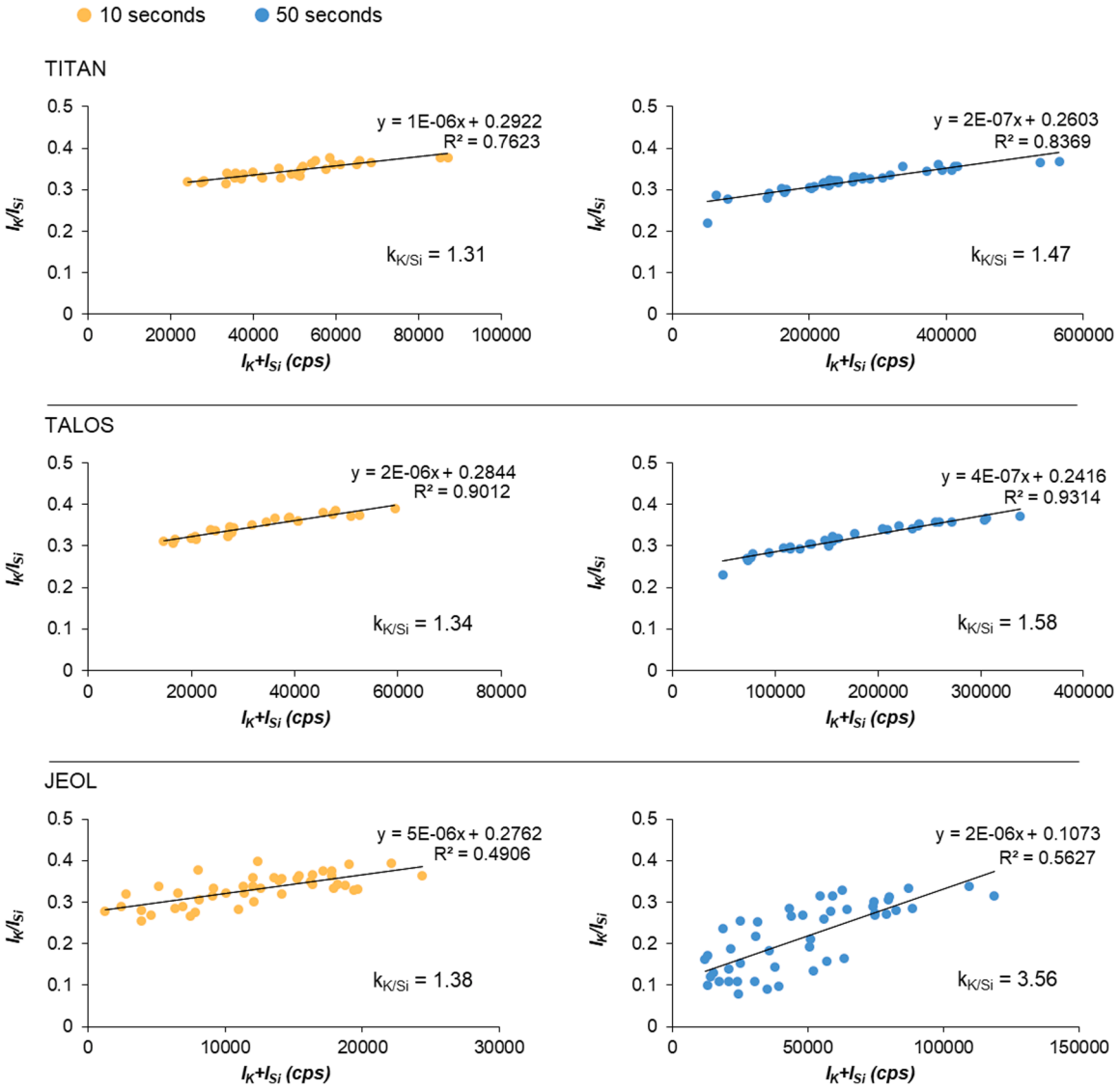

Fig. 3. I_K/I_{Si} vs. I_K+I_{Si} intensities in muscovite at both 10 and 50 s for the TITAN, TALOS and JEOL instruments.

corners above the sample and an overall detection solid angle larger than the JEOL, which has only one sensitive SDD. Therefore, the TALOS and the TITAN have a more efficient system for collecting X-ray photons, resulting in better counting statistics, higher precision and possibly higher sensitivity.

Regarding the radiation-induced migration of monovalent cations, it is evident that the redistribution of K is significant with longer acquisition times, as evidenced by the systematically smaller relative intensities resulting from 50 s acquisitions (net time). Surprisingly, it is greater in the JEOL than in the TALOS and TITAN, when one would

expect the opposite. Indeed, this effect in microprobe analysis is primarily caused by the energy released to the sample atoms by the electron beam. Field emission gun source systems, such as those equipping the TALOS and the TITAN, are considered to be more brilliant (and coherent) than thermionic sources, like the LaB_6 gun equipping the JEOL, as actually confirmed by the measured beam currents. However, the nominal spot size for the JEOL was 3 nm, whereas that of the TALOS and TITAN was 5 nm, leading to a current density of 49, 24 and 36 pA·nm^2, respectively. Therefore, the electron dose per atom was higher for the JEOL than for the FEG instruments, explaining the apparent inconsistency.

Conconi et al. [5] showed how the determination of the $k_{O/Si}$ is complicated by the scattered values of the O data, which are affected by the low energy/high absorption of the $O_{K\alpha}$ radiation. For this reason, two different $k_{O/Si}$ values were required: one for denser phases and the other for lighter ones, with a threshold at 2.90 g/cm^3. The same is observed here for the TITAN and TALOS instruments, with some anomalies. For the TALOS, the $k_{O/Si}$ values for the lighter phases (albite, anorthite, anorthoclase, biotite, microcline, muscovite and osumilite) range from 0.84 to 1.15, while those of the denser phases (augite, spessartine, hemimorphite, rhodonite, olivine and titanite) range from 1.08 to 1.23 (for hemimorphite, density ~3.48, the $k_{O/Si} = 1.08$ is lower than expected). In the TITAN, the $k_{O/Si}$ values for the lighter phases range from 1.30 to 1.49, while those of the denser phases range from 1.30 to 1.78 (for spessartite, density = 4.12–4.32, $k_{O/Si} = 1.30$ is lower than expected). For the JEOL [5], the $k_{O/Si}$ values for the lighter phases range from 1.15 to 1.38, while those of the denser phases range from 1.42 to 1.57 (for osumilite, density = 2.58–2.68, $k_{O/Si} = 1.43$, is higher than expected). Contrary to what was observed with the JEOL instrument and discussed in Conconi et al. [5], the $k_{Cr/Si}$ factors for the TITAN and TALOS instruments are not overestimated. These anomalies cannot be explained in a simple way, except by admitting some inhomogeneity in the standards.

3.2. *Application to reference samples*

TEM-EDS results on the same reference samples analysed by Conconi et al. [5], namely johannsenite, antigorite, biotite, cordierite, fayalite and spinel, are reported in Figs. 4 and 5 and in the Supplementary Materials (Table S3). Generally, the absorption correction method

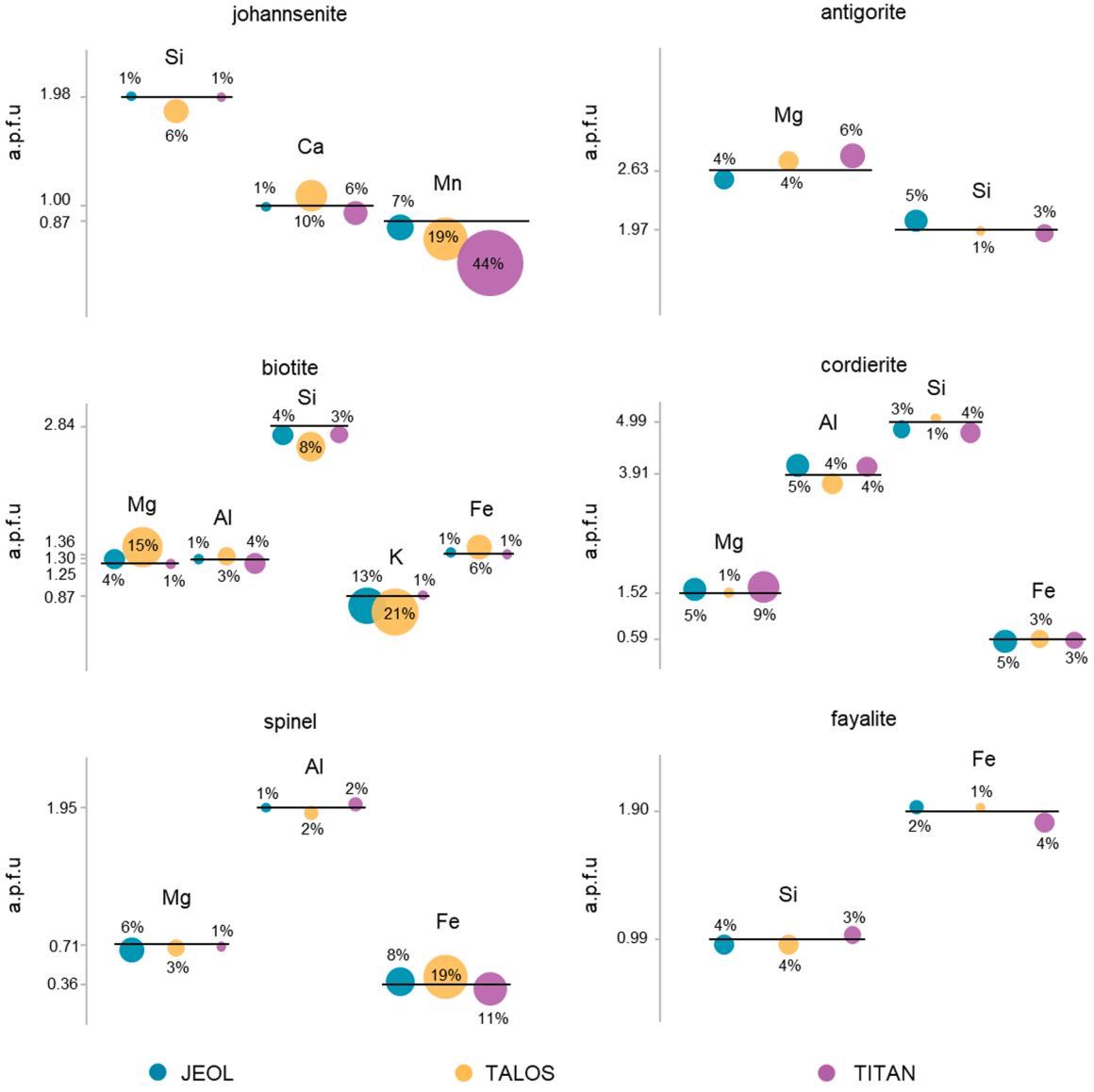

Fig. 4. Deviations (%) of the analyses obtained with the ACM from the compositions of several reference minerals, the horizontal lines represent the concentration of the elements in the reference material.

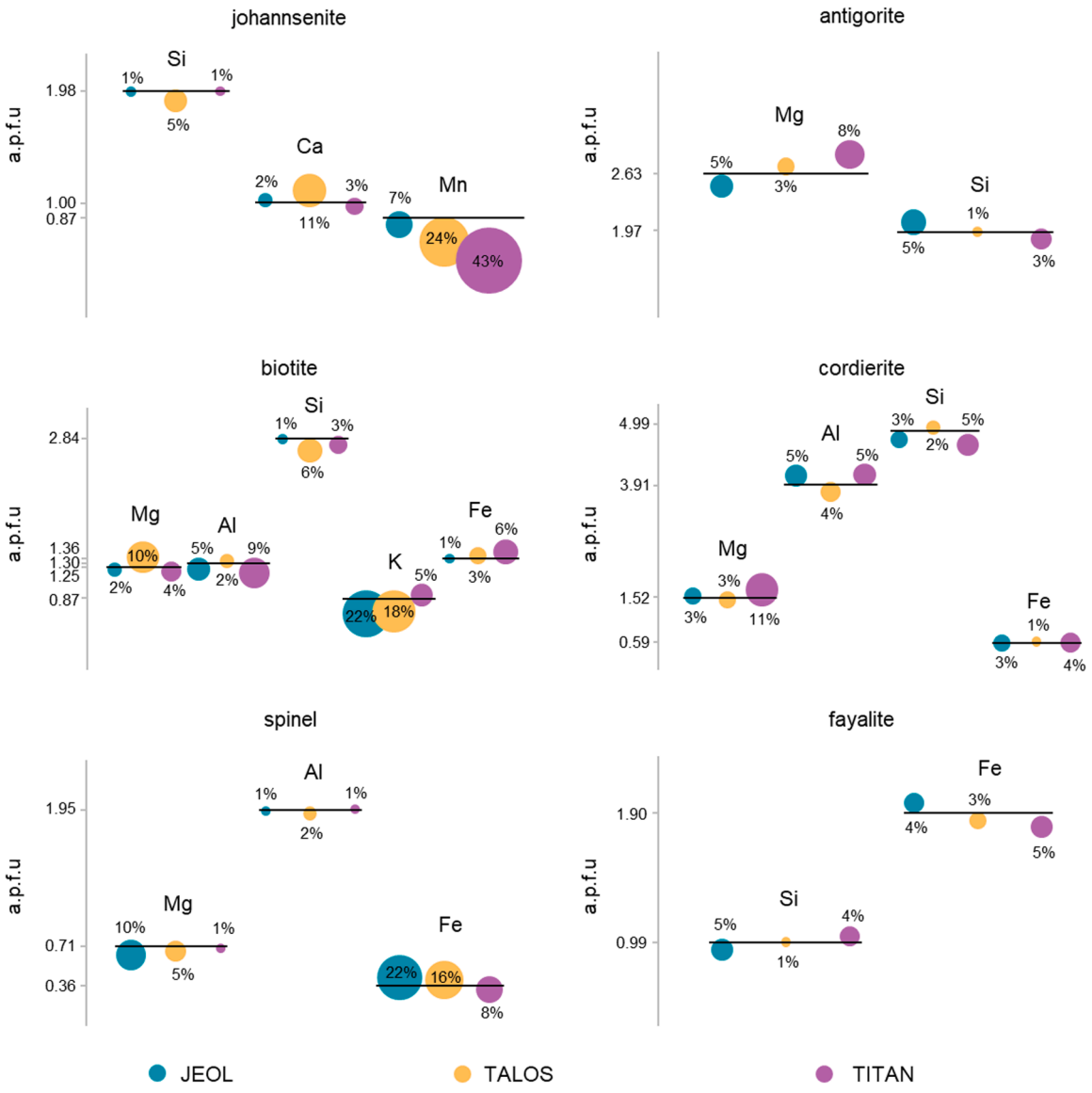

Fig. 5. Deviations (%) of the analyses obtained with the CLA from the compositions of several reference minerals, the horizontal lines represent the concentration of the elements in the reference material.

returns slightly better results than the Cliff-Lorimer approximation. Overall, the results show that deviations from the reference samples are below 10 % (and generally much smaller) for major elements. Exceptions concern Mn in johannsenite, K in biotite and Fe in spinel, which show deviations from the reference as high as 43 %, 22 % and 22 %, respectively (Fig. 5). As discussed in Conconi et al. [5], these large deviations are due to intrinsic issues with the reference samples, namely chemical zoning in johannsenite and radiation-induced migration of K atoms and channelling effects in biotite. The 22 % deviation in Fe content in spinel, corresponding to 0.08 atom per formula unit (a.p.f.u.) from the reference value of 0.36, which in turn is well above (~13 wt %) the commonly accepted detection limit of TEM-EDS (1–0.1 wt %), it cannot be easily explained (see below).

Some discrepancies arise among the analyses performed with the three microscopes. Considering fayalite (Table 1 and Table S3), Fe and Si should be present at 1.90 and 0.99 a.p.f.u., respectively. However, when applying the Cliff-Lorimer approximation, the resulting Fe values are 1.97, 1.85, and 1.80 a.p.f.u. for the JEOL, TALOS, and TITAN, respectively, while the corresponding Si values are 0.94, 0.99, and 1.03. Clearly, Fe is overestimated in the JEOL and underestimated in the

Table 1
Comparison of fayalite analyses for the JEOL, TALOS and TITAN, quantified using the Aztec, Velox and HyperSpy programs using the absorption correction method. In bold the deviations from the reference analysis.

		JEOL				TALOS				TITAN			
	Reference	HyperSpy		Aztec		HyperSpy		Velox		HyperSpy		Velox	
Mg	0.03	0.035	**15.33 %**	0.031	**3.89 %**	0.029	**2.71 %**	0.032	**7.99 %**	0.023	**23.82 %**	0.030	**1.52 %**
Si	0.99	0.967	**2.35 %**	0.952	**3.89 %**	0.985	**0.50 %**	0.949	**4.13 %**	0.998	**0.86 %**	1.024	**3.45 %**
Mn	0.09	0.097	**7.65 %**	0.103	**14.01 %**	0.081	**10.29 %**	0.100	**11.11 %**	0.083	**7.46 %**	0.097	**7.78 %**
Fe	1.90	1.899	**0.08 %**	1.927	**1.40 %**	1.882	**0.97 %**	1.927	**1.44 %**	1.883	**0.90 %**	1.825	**3.97 %**

TALOS and TITAN, whereas Si is underestimated in the JEOL. These discrepancies primarily result from X-ray absorption, which can significantly impact quantification, especially in high density phases like fayalite and when the sample thickness is not thin enough [5].

After correcting for absorption, the Fe and Si values improve to 1.93, 1.93, and 1.82 a.p.f.u. for Fe, and 0.95, 0.95, and 1.02 a.p.f.u. for Si, across the JEOL, TALOS and TITAN microscopes, respectively. These values are in much better agreement with the reference values (except for Fe in the TITAN) even though some minor discrepancies persist.

To more accurately compare results from the three microscopes and eliminate any differences introduced by the software (i.e., Aztec and Velox), a new set of 0 thickness extrapolated *k*-factors was derived using a HyperSpy Python script (Table S4) [16]. All spectra were processed (background removal and peak fitting) and quantified with the absorption correction method using the same script. The resulting analyses generally yield improved results compared to those obtained using either Velox or Aztec. Specifically, for high-concentration elements such as Si and Fe, the compositions obtained with HyperSpy more closely match the reference values than those from Velox or Aztec. Indeed, the deviation from the reference value decreases in all cases (Table 1). In contrast, for low-concentration elements like Mg and Mn, the results show larger deviations in the HyperSpy measurements. The larger deviations for Mg analyses are not surprising, given the low concentration of the element. For example, in both the JEOL and TITAN instruments, deviations of 15.33 % and 23.82 % from the reference value correspond to absolute differences of only 0.005 and 0.007 a.p.f.u., respectively. For an element with a concentration of approximately 0.4 wt %, these values are far below the detection limit.

The detection limits of the three systems were evaluated by examining minor elements (< 1 wt %) in the reference samples. As expected, the detection limit is lower in the 4 in-column SDD systems than in the classical single SDD system. Minor elements are consistently detected with the 4 in-column SDD systems, whereas this is not always the case for the single SDD detector (e.g., Al in johannsenite, Ca in biotite and Mn in cordierite; see Table S3 in Supplementary Material). However, these results may be influenced by the different ways the different systems (Velox, Aztec) adopt to process the spectra. Therefore, to avoid such influence, spectra collected for fayalite with the three different instruments were processed with HyperSpy.

Fig. 6 illustrates the relative error trends in the three instruments for three different elements: Fe, Mn and Mg, which exhibit different concentrations in fayalite. Indeed, Fe is a major element with concentration ~50 wt %, Mn is a major element with concentration ~2.7 wt % and Mg is a minor element with concentration ~0.4 wt %. Overall, the error associated with the analysis decreases when the thickness increases for all three instruments, reflecting the increase of the peak-to-background ratio with increasing sample thickness; as expected, it is lower for abundant elements (Fe and Mn, in the order) and higher for scarce elements (Mg).

4. Conclusions

A first conclusion drawn from this comparison is that EDS calibration appears to be "strictly instrument specific". Even among TEMs equipped with identical EDS systems, specific calibration is necessary. Numerous published *k*-factors are available for different accelerating voltages, reference elements and X-ray lines; see Williams and Carter [2] and references therein. This study demonstrates, if any doubt remained, that universally valid *k*-factors cannot exist.

Another conclusion is that 4-in column SDD systems are more efficient in data collection, enabling more precise *k*-factors and lower detection limits. However, the comparison between the performance of classic single SDD system (Oxford/JEOL) and modern 4 in-column SDD systems (Thermofisher/TALOS and TITAN) does not unequivocally favour the latter in terms of final accuracy. This suggests that other error sources may influence the outcome, such as the quality of the standards and the complexity and diversity of natural minerals in terms of chemistry, density, matrix effects, etc.

As anticipated, the detection limit is lower for 4 in-column SDD systems than for classical single SDD systems. Conversely, EDS analyses performed in both TALOS and TITAN exhibit lower radiation-induced migration of weakly bounded elements – as K in phyllosilicates, for instance – than those obtained with the JEOL. In the present case, the result can be explained considering the smaller spot size used with the conventional TEM, that in total led to a higher electron dose per atom for the latter than for the FEG instruments.

This work confirms that the absorption correction method proposed by Van Cappellen and Doukhan [7] should be the preferred tool whenever dealing with thicker and/or dense samples, whereas the Cliff and Lorimer approximation [6], since simpler and faster, in all the other cases. The superiority of both the above methods over the standardless approach [4] was previously established by Conconi et al. [5] and not further investigated here. Additionally, this study confirms the necessity to determine (at least) two distinct $k_{O/Si}$ factors, one for lighter and one

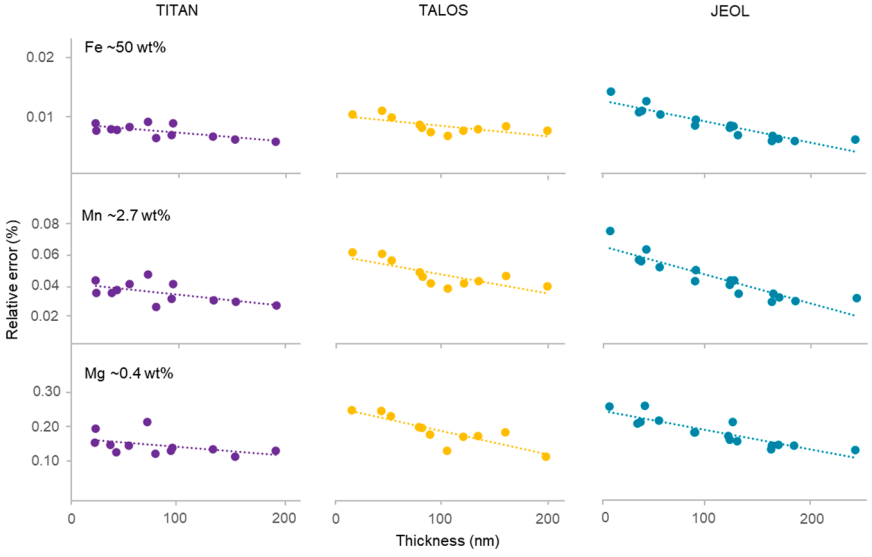

Fig. 6. Relative error(%) trend in the three instruments for Fe, Mn and Mg in fayalite. The net and background intensities used to calculate the relative error were obtained from spectra processed with HyperSpy.

for denser compounds, and highlights some anomalies in the response of few mineral standards in this context.

Finally, the challenges encountered in deriving *k*-factors from minerals with very different structure/chemistry, as exemplified in the case of $k_{Cr/Si}$ in [5], were not particularly pronounced here. However, the feeling remains that more accurate EDS quantification could be achieved through distinct *k*-factors data sets for the major and diverse mineral classes.

CRediT authorship contribution statement

Roberto Conconi: Writing – original draft, Validation, Methodology, Investigation, Data curation, Conceptualization. **María del Mar Abad Ortega:** Methodology, Investigation. **Fernando Nieto:** Supervision, Resources. **Paolo Buono:** Software. **Giancarlo Capitani:** Writing – original draft, Validation, Supervision, Resources, Conceptualization.

Declaration of competing interest

The authors declare that they have no known competing financial interests or personal relationships that could have appeared to influence the work reported in this paper.

Acknowledgements

Cecilia de la Prada Sánchez is greatly acknowledged for her help during TEM analysis at the Centro de Instrumentación Científica of the University of Granada. The Platform of Microscopy of Milano-Bicocca has been co-funded by the Dipartimenti di Eccellenza 2018-2023 and 2023-2027 grants. Constructive comments by Bernard Grobéty and two anonymous reviewers greatly helped to improve the manuscript.

Supplementary materials

Supplementary material associated with this article can be found, in the online version, at doi:10.1016/j.ultramic.2025.114201.

Data availability

Data will be made available on request.

References

[1] K.F.J. Heinrich, H. Yakowitz, Absorption of primary X rays in electron probe microanalysis, Analyt. Chem. 47 (1975).
[2] D.B. Williams, C.B. Carter, Transmission Electron Microscopy: A Textbook For Materials Science, Springer US, Boston, MA, 1996.
[3] D.E. Newbury, C.R. Swyt, R.L. Myklebust, Standardless" quantitative electron probe microanalysis with energy-dispersive X-ray spectrometry: is it worth the risk? Anal. Chem. 67 (1995) 1866–1871.
[4] D.E. Newbury, Standardless quantitative electron-excited X-ray microanalysis by energy-dispersive spectrometry: what is its proper role?, microsc, Microanal 4 (6) (1998) 585–597, https://doi.org/10.1017/S1431927698980564.
[5] R. Conconi, G. Ventruti, F. Nieto, G. Capitani, TEM-EDS microanalysis: comparison among the standardless, Cliff & Lorimer and absorption correction quantification methods, Ultramicroscopy 254 (2023) 113845, https://doi.org/10.1016/j.ultramic.2023.113845.
[6] G. Cliff, G.W. Lorimer, The quantitative analysis of thin specimens, J. Microsc. 103 (1975) 203–207, https://doi.org/10.1111/j.1365-2818.1975.tb03895.x.
[7] E. van Cappellen, J.C. Doukhan, Quantitative transmission X-ray microanalysis of ionic compounds, Ultramicroscopy 53 (1994) 343–349.
[8] M. Watanabe, Z. Horita, M. Nemoto, Absorption correction and thickness determination using ζ-factor in quantitative X-ray microanalysis, Ultramicroscopy 65 (1996) 187–198, https://doi.org/10.1016/S0304-3991(96)00070-8.
[9] M. Watanabe, D.B. Williams, The quantitative analysis of thin specimens: a review of progress from the Cliff-Lorimer to the new zeta-factor methods, J. Microsc. 211 (2006) 89–109, https://doi.org/10.1111/j.1365-2818.2006.01549.x.
[10] W.J. Moon, S.G. Yu, Y.S. Kim, B.K. Park, W.G. Jung, H.J. Song, New strategy to improve the accuracy of quantitative analysis of energy dispersive spectroscopy, Phys. Scr. 99 (2024) 035013, https://doi.org/10.1088/1402-4896/ad241e.
[11] K. Fujino, N. Tomioka, H. Ohfuji, New approach to obtain the correct chemical compositions by absorption correction using analytical transmission electron microscopy, J. Mineral. Petrol. Sci. 118 (2023) 221017, https://doi.org/10.2465/JMPS.221017.
[12] E. Sanità, R. Conconi, M.Di Rosa S.Lorenzon, G. Capitani, E. Mugnaioli, Application of an improved TEM-EDS protocol based on charge balance for accurate chemical analysis of sub-micrometric phyllosilicates in low-grade metamorphic rocks, Clays. Clay. Miner. 72 (2025) e31, https://doi.org/10.1017/cmn.2024.32.
[13] N.J. Zaluzec, Analytical formulae for calculation of X-ray detector solid angles in the scanning and scanning/transmission Analytical electron microscope, Microsc. Microanal. 20 (2014) 1318–1326, https://doi.org/10.1017/S1431927614000956.
[14] N.J. Zaluzec, Quantitative assessment and measurement of X-ray detector performance and solid angle in the analytical electron microscope, Microsc. Microanal. 28 (2022) 83–95, https://doi.org/10.1017/S143192762101360X.
[15] P.T. Pinard, A. Protheroe, J. Holland, S. Burgess, P.J. Statham, Development and validation of standardless and standards-based X-ray microanalysis, in: IOP Conf. Ser.: Mater. Sci. Eng. 891, 2020 012020, https://doi.org/10.1088/1757-899X/891/1/012020.
[16] F. de la Peña, T. Ostasevicius, V.T. Fauske, P. Burdet, P. Jokubauskas, M. Nord, M. Sarahan, M.E. Prestat, D.N. Johnstone, J. Taillon, J. Caron, T. Furnival, K. E. MacArthur, A. Eljarrat, S. Mazzucco, V. Migunov, T. Aarholt, M. Walls, F. Winkler, G. Donval, B. Martineau, A. Garmannslund, L.F. Zagonel, I. Iyengar, Electron microscopy (Big and Small) data analysis with the open source software package HyperSpy, Microsc. Microanal. 23 (2017) 214–215, https://doi.org/10.1017/s1431927617001751.
[17] P.M. Zanetta, C. Le Guillou, H. Leroux, B. Zanda, R.H. Hewins, E. Lewin, S. Pont, Modal abundance, density and chemistry of micrometer-sized assemblages by advanced electron microscopy: application to chondrites, Chem. Geol. 514 (2019) 27–41, https://doi.org/10.1016/j.chemgeo.2019.03.025.
[18] HyperSpy User Manual. https://hyperspy.org/hyperspy-doc/current/user_guide/index.html, 2025 (accessed 12 February 2025).